Neutron-Excess Dependence of Fusion—Ni + Sn

W. S. Freeman, H. Ernst,[a] D. F. Geesaman, W. Henning, T. J. Humanic,[b] W. Kühn,[c] G. Rosner, J. P. Schiffer, and B. Zeidman
Argonne National Laboratory, Argonne, Illinois 60439

and

F. W. Prosser
University of Kansas, Lawrence, Kansas 66045

(Received 21 March 1983)

Excitation functions (E_{lab} = 235–320 MeV) for producing nuclei close to the compound system (evaporation residues) were measured for $^{58,64}Ni + ^{112-124}Sn$, corresponding to a 20% variation in the compound-nucleus neutron number. A dramatic, order-of-magnitude increase was observed in the maximum cross section as a function of the compound-nucleus neutron excess. The subbarrier energy dependence of the cross sections is well described by an optical-model calculation, but not by the frequently used parabolic approximation.

PACS numbers: 25.70.Jj, 25.70.Gh

Considerable theoretical and experimental effort has focused recently on fusion reactions in moderately heavy systems (compound nuclei with $A \gtrsim 160$). Points of particular interest include (i) the subbarrier energy dependence of cross sections,[1-5] (ii) the competition between the survival of the compund nucleus leaving an evaporation residue, σ_{ER}, and fission,[6,7] and (iii) the possible requirement of an "extra-push" energy to achieve fusion in heavy systems.[8,9] Identification of the evaporation residues, left after light-particle evaporation from the compound nucleus, represents an unambiguous signature of fusion. This Letter reports measurments of cross sections for $^{58,64}Ni$ fusing with the even-mass Sn isotopes (A = 112–124) at energies ranging from below the classical fusion barrier to well above it. The choice of Sn as the target material allowed a systematic study of the target (and compound nucleus) neutron-number dependence of σ_{ER}. The compund nuclei span the range from the very-proton-rich ^{170}Pt to ^{188}Pt, a change of 18 neutrons or ~20% in neutron number.

For such heavy systems, direct measurements of σ_{ER} are complicated by the fact that the angular distributions are strongly forward peaked. Measurements must be made at angles well inside 5°, where the counting rate from elastic scattering is high. In addition, σ_{ER} may be small, either because the bombarding energy is well below the classical fusion barrier, or because of fission. For these reasons, several laboratories have utilized recoil-mass separators or velocity filters to reduce the background.[10-12] In the present measurements, the nuclei emerging from the target at ~0° were separated from the beam (and small-angle elastic scattering) by an electrostatic deflector. The separated evaporation residues were then identified by their energy loss and residual energy in a ΔE-E detector assembly.

The isotopically enriched targets (250–300 $\mu g/cm^2$ Sn evaporated on 20-$\mu g/cm^2$ C backings) were positioned in front of the entrance to a 1.7-m-diam scattering chamber with the deflector (25 cm long × 3 cm plate separation, V_{max} ~45 kV) 25 cm further downstream. The entrance to the deflector was restricted by a vertical slit to particles scattered at the target by less than ±1° in the deflection plane. This enabled the detection of evaporation residues without requiring a substantial reduction in incident beam current (typical values were 1–2 particle nA).

The ΔE-E detector consisted of up to four silicon surface-barrier E detectors inside a common ΔE gas ionization chamber. The silicon detectors were arranged to measure the angular distributions *vertically* (perpendicular to the deflection plane) up to a maximum angle of 3.1°. Each detector subtended a solid angle of 0.22 msr defined by a circular aperture at the entrance to the ΔE gas volume. The target-to-detector distance of 1.78 m corresponded to a flight time of ~180 nsec for a 90-MeV, A = 180 evaporation residue. The electric field strength of the deflector was selected to maximize the yield from each target, while the relative and absolute cross sections were obtained by normalizing the measurements to Rutherford scattering in a silicon monitor counterfixed at a forward angle. Angle-integrated cross sections were extracted by fitting the angular distributions with Gaussian shapes whose centroids were kept fixed at 0°. All the measurements reported here used ^{58,64}Ni beams of 235–320 MeV from the Argonne superconducting linac.

Monte Carlo ray-tracing calculations of the effective detector efficiencies relative to the geometric solid angles resulted in small (10%) corrections to the data. The calculations included as parameters the evaporation-residue angular distributions ($\Delta\theta \sim 2.2°$ full width at half maximum), the beam spot size (~3 mm), and reasonable estimates of the atomic charge-state distribution and kinetic energy spread of the nuclei ($\Delta Q/Q \sim 20\%$, $\Delta E/E \sim 12\%$). Doubling the assumed width of the charge-state distribution decreases the calculated efficiency by an additional 10%, and this uncertainty is included in the estimated ±20% overall systematic uncertainty of the cross sections. The beam energies are accurate to ±1 MeV.

The excitation functions for ^{58,64}Ni + Sn are shown in Fig. 1. The cross sections for all targets rise steeply from a center-of-mass energy of ~150 MeV and then flatten out near 170–180 MeV, with perhaps a slight decrease toward higher energies. The most striking feature of the data is the increase of one order of magnitude in the maximum cross section as one goes from the most proton-rich compound nucleus ^{170}Pt to the most neutron-rich nucleus ^{188}Pt. Qualitatively, this might reflect both changes in the compound-nucleus cross sections and changes in the fission competition. Assuming equal compound-nucleus cross sections of 300 mb at $E_{\mathrm{c.m.}} = 180$ MeV for all systems (obtained from the extra-push model[8] for ^{58}Ni + ^{124}Sn), we calculated the evaporation-residue cross sections using the statistical-model code CASCADE.[13] The solid (broken)-line histogram in Fig. 2 is the calculated result σ_{ER} for ^{64}Ni (^{58}Ni). It is important to note that the calculated results are insensitive to the exact choice of compound-nucleus cross section as long as a reasonably sharp cutoff in angular momentum is assumed, since at this energy the calculation shows that the higher partial waves all decay via the fission channel. While the qualitative trend of increasing evaporation-residue cross sections with increasing neutron numbers is also a feature of the calculation, it is apparent that there are some significant differences not contained within the calculations. For ^{64}Ni, the calculated cross sections are systematically lower than the data and the A dependence in the data is slightly greater than in the calculations. The magnitudes of calculated cross sections are in somewhat better agreement with the data for ^{58}Ni, though they again fail to reproduce the increase between the compound nuclei with A of 170 and 182; the calculations yield a factor of ~2 while the observed increase is ~3.2 ± 0.7. For the lightest systems studied here σ_{ER} is no more than 10% of the compound-nucleus cross

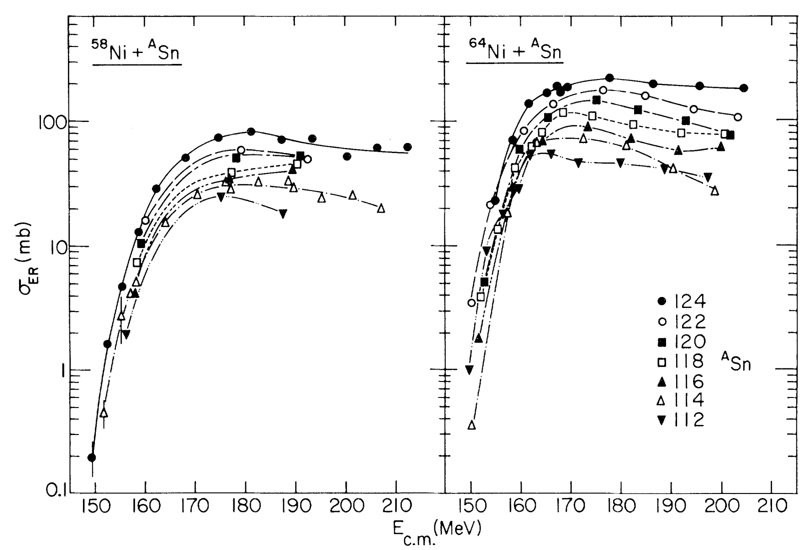

FIG. 1. Values of the fusion cross section leaving evaporation residues for ^{58,64}Ni fusing with the even-mass Sn isotopes ($A = 112$–124). The symbols designating the cross sections for each target are given in the figure. Lines are drawn only to guide the eye.

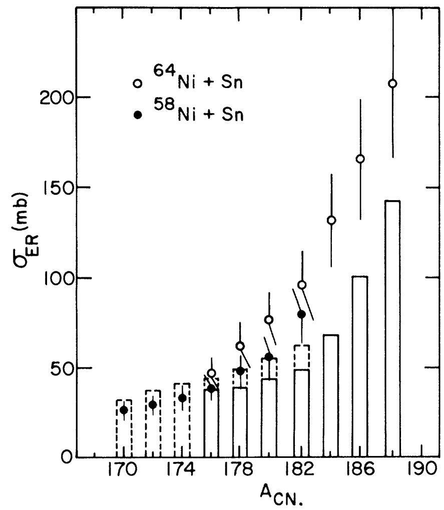

FIG. 2. Values of σ_{ER} as a function of the compound-nucleus mass for ^{58,64}Ni + Sn at $E_{c.m.} = 180$ MeV. The open (filled) circles denote ^{64}Ni (^{58}Ni) as the projectile. The error bars reflect ±20% systematic uncertainties in the overall cross-section normalizations; the relative target to target uncertainties are somewhat smaller (~15%). The solid (broken)-line histograms are the results of statistical-model calculations with ^{64}Ni (^{58}Ni) as the projectile. Rotating–liquid-drop fission barriers were assumed with the level density parameters given by $a_f/a_n = 1.0$.

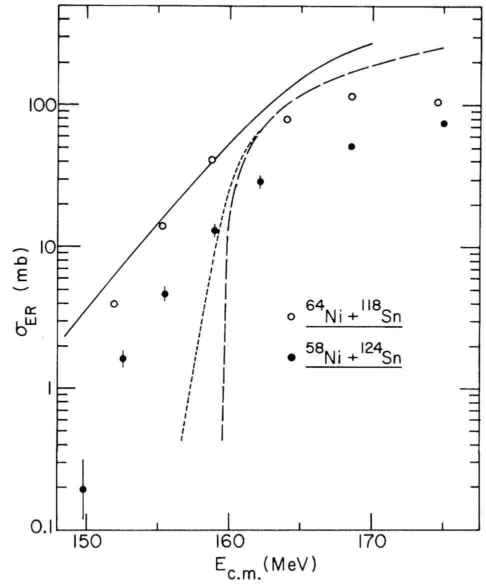

FIG. 3. Values of σ_{ER} in the subbarrier region for ^{58}Ni + ^{124}Sn (filled circles) and ^{64}Ni + ^{118}Sn (open circles), compared with optical-model reaction cross sections (solid line), the extra-push model (long-dashed line), and a Hill-Wheeler barrier-penetration calculation (short-dashed line). Error bars denote statistical uncertainties only. Optical-model parameters: $V = 58.1$ MeV, $W = 62.9$ Mev, $r_R = r_I = 1.26$ fm, $a_R = a_I = 0.294$ fm.

section, and the calculated results are sensitive to small changes in the statistical-model parameters. For example, increasing the height of the L-dependent fission barriers above the value obtained from the rotating–liquid-drop model doubles the calculated σ_{ER} for ^{64}Ni + ^{112}Sn, in complete disagreement with the data. A similar increase for ^{64}Ni + ^{124}Sn, however, results in better agreement. As has been recently pointed out by Blann *et al.*,[7] precise measurements of σ_{ER} at sufficiently high energies (where $\sigma_{fiss} \gg \sigma_{ER}$) may be the most sensitive test of fission parameters in statistical-model calculations.

In the subbarrier energy region, we see that the excitation functions for all targets have similar energy dependences, and that they agree reasonably well with the energy dependence of the reaction cross section calculated with an optical model.[14] In Fig. 3, we show such a calculation for ^{58}Ni + ^{124}Sn compared with the data for ^{58}Ni + ^{124}Sn and ^{64}Ni + ^{118}Sn which form the same compound nucleus, ^{182}Pt. The optical-model parameters were obtained by fitting real and imaginary Woods-Saxon potentials of the same radius and diffuseness to a (quasi)elastic scattering angular distribution at $E_{lab} = 278$ MeV. On the other hand, the energy dependence predicted by a typical, one-dimensional parabolic barrier-penetration calculation (short-dashed line, Fig. 3) fails to reproduce the slope of the data below the barrier and underestimates the cross section by more than an order of magnitude at $E_{c.m.} \approx 156$ MeV. This latter calculation followed the procedure of Beckerman *et al.*,[3] where Hill-Wheeler transmission coefficients, which describe the penetration through a real, inverted parabolic barrier, were used. Such transmission coefficients deviate from the optical-model ones at far subbarrier energies. For comparison with a classical model that does not include barrier penetration, we also show the prediction of the extra-push model of Swiatecki for ^{58}Ni + ^{124}Sn using the parameters of Ref. 8.

The usual, intuitive picture of the fusion process is that of penetration through or over a (real) potential barrier with subsequent absorption in the nuclear interior. To assess the impact of this assumption the same reaction-cross-section calculations were repeated with the imaginary potential radii reduced by 0.5 and 1.0 fm. The changes in the energy dependence of the cross section were small and in all cases gave a slope considerably less steep than the parabolic approximation and in better agreement with the data.

To summarize, we have measured σ_{ER} for ^{58,64}Ni bombarding the even-mass Sn isotopes over a wide range of incident energies. These data constitute the first systematic study of this macroscopic property of heavy-ion reactions over a wide range of neutron excess and energy. The cross sections for all targets reached their maximum values between 170 and 180 MeV (c.m.) and decreased slightly at higher energies. The energy dependences of the subbarrier cross sections were similar for all targets, and consistent with optical-model calculations. Above the barrier, a strong target (and compound-nucleus) dependence of the cross sections was observed which was similar to the predictions of a statistical model that included fission competition, but significantly greater in magnitude. Such trends should lead to a bettter understanding of the dynamics of heavy-ion reactions.

This work was supported by the U. S. Department of Energy under Contracts No. W-31-109-Eng-38 and No. DE-AC02-79ER10420.

[(a)]Present address: Technische Universität, München, West Germany.
[(b)]Present address: Lawrence Berkeley Laboratory, Berkeley, Cal. 94720.
[(c)]Present address: University of Giessen, Giessen, West Germany.

[1]R. G. Stokstad, W. Reisdorf, K. D. Hildenbrand, J. V. Kratz, G. Wirth, R. Lucas, and J. Poitou, Z. Phys. A 295, 269 (1980).

[2]W. Reisdorf, F. P. Hessberger, K. D. Hildenbrand, S. Hofman, G. Münzenberg, K.-H. Schmidt, J. H. R. Schneider, W. F. W. Schneider, K. Summerer, G. Wirth, J. V. Kratz, and K. Schlitt, Phys. Rev. Lett. 49, 1811 (1982).

[3]M. Beckerman, J. Ball, H. Enge, M. Salomaa, A. Sperduto, S. Gazes, A. DiRienzo, and J. D. Molitoris, Phys. Rev. C 23, 1581 (1982).

[4]M. Beckerman, M. Salomaa, A. Sperduto, J. D. Molitoris, and A. DiRienzo, Phys. Rev. C 25, 837 (1982).

[5]M. Beckerman, M. K. Salomaa, J. Wiggins, and R. Rohe, Phys. Rev. Lett. 50, 471 (1983).

[6]B. Sikora, W. Scobel, M. Beckerman, J. Bisplinghoff, and M. Blann, Phys. Rev. C 25, 1446 (1982).

[7]M. Blann, D. Akers, T. A. Komoto, F. S. Dietrich, L. F. Hansen, J. G. Woodworth, W. Scobel, J. Bisplinghoff, B. Sikora, F. Plasil, and R. L. Ferguson, Phys. Rev. C 26, 1471 (1982).

[8]W. J. Swiatecki, Phys. Scr. 24, 113 (1981), and Nucl. Phys. A376, 275 (1982).

[9]S. Bjørnholm and W. J. Swiatecki, Nucl. Phys. A391, 471 (1982).

[10]M. Salomaa and H. A. Enge, Nucl. Instrum. Methods 145, 279 (1977); H. A. Enge and D. Horn, Nucl. Instrum. Methods 145, 271 (1977).

[11]G. Münzenberg, W. Faust, S. Hofmann, P. Armbruster, K. Güttner, and H. Ewald, Nucl. Instrum. Methods 161, 65 (1979).

[12]T. Cormier and P. M. Stwertka, Nucl. Instrum. Methods 184, 423 (1981).

[13]F. Pühlofer, Nucl. Phys. A280, 267 (1977).

[14]M. H. Macfarlane and S. C. Pieper, Argonne National Laboratory Report No. ANL-76-11, 1976 (unpublished).